

# Fast response ZnO:Al/CuO nanowire/ZnO:Al heterostructure light sensors fabricated by dielectrophoresis

A. García Marín,<sup>a)</sup> C. García Núñez, E. Ruiz, J. Piqueras, and J. L. Pau  
*Laboratorio de Microelectrónica, Grupo ELYSE, Dpto. Física Aplicada, Facultad de Ciencias,  
 Universidad Autónoma de Madrid, 28049 Madrid, Spain*

(Received 8 March 2013; accepted 29 May 2013; published online 12 June 2013)

Metal oxide nanowire (NW) photoconductors tend to exhibit high photoconductive gains and long recovery times mainly due to surface effects. In this work, p-type CuO NWs are synthesized by direct oxidation of copper and deposited on n-type ZnO:Al electrodes by dielectrophoresis. The heterostructure is electro-optically characterized showing recovery times in the 10  $\mu$ s range, mainly limited by the resistance-capacitance product of the equivalent circuit, without signs of persistent effects. The fast response is attributed to short transit times across space charge regions built between CuO and ZnO:Al materials and fast carrier recombination at neutral regions. © 2013 AIP Publishing LLC. [<http://dx.doi.org/10.1063/1.4811128>]

Metal oxides (MOs) are attractive compounds for industrial purposes since high-quality crystal nanowires (NWs) can be obtained by cost-effective methods that do not require expensive vacuum systems or environmentally unfriendly chemical reactants. The high surface-to-volume ratio of such nanostructures leads to the enhancement of the device sensitivity prompting their use as building blocks in low-cost optical, biological, and gas sensors.<sup>1–4</sup> Regarding light detectors, NWs may help to reduce the operation voltages of high-gain sensors through the proximity of the surface and the subsequent enhancement of the local electric field. In addition, their small dimensions open possibilities for the integration of NWs from different materials or with different structures such as core-shell, p-n junctions, or quantum well superlattices.<sup>5,6</sup>

However, the development of NW-based devices has to face issues such as the lack of performance reproducibility or the need for advanced methods to handle and manipulate nanostructures on a high demand basis. Dielectrophoresis (DEP) has long been used in biochemistry to separate biomolecules, but nowadays, it has also been proved to be a cost-effective technique to align NWs between metal electrodes.<sup>7,8</sup> The technique is highly scalable and makes possible the precise placement of multiple NWs on Si integrated circuits at room temperature. Thus, ZnO NW devices have been fabricated using this method on Au electrodes.<sup>9</sup> Due to their high conductance and mechanical stability, Al-doped ZnO (AZO) is an alternative material to metals for the preparation of DEP electrodes. Moreover, its visible transparency also enables the alignment of NWs on desired locations of transparent substrates aiming at the development of sensors in transparent electronics.

Concerning the performance of NW devices, the understanding of the surface effects is crucial since many of the electrical and optical characteristics are strongly influenced by surface electronic states. On many MO-NW light sensors, these surface effects lead to obtain photoresponse values well beyond those achieved in mesoscopic devices, at the

expense of showing long recovery times.<sup>10,11</sup> Unfortunately, these slow transients hinder their practical application in many fields.

Recently, p-type cupric oxide (CuO) NWs have received a great deal of attention because of their high performance as part of gas sensor devices.<sup>6,12</sup> Its optical bandgap lies in the infrared range (1.2–1.4 eV) allowing detection in the full visible spectrum.<sup>13–15</sup> Different growth methods have been used for the synthesis of CuO NWs, such as chemical,<sup>16</sup> template-assisted techniques,<sup>2</sup> or direct oxidation of regular Cu foils.<sup>17–19</sup> The latter has been demonstrated to be an easy and cost-effective method where no catalysts are needed. In this paper, we are reporting the synthesis of p-type CuO NWs and their deposition on n-type AZO electrodes by alternating current (AC) DEP. Resultant structures are electro-optically characterized to investigate their potential use in light sensor devices.

Prior to growth, 99.98% pure Cu foils (Sigma-Aldrich) were dipped in ethanol, sonicated for 2 min to remove adsorbed impurities, and blown with dry nitrogen. Then, the foils were placed on a hot plate at 410 °C and oxidized in air ambient during 1 h, leaving the sample on the unheated plate overnight for cooling down. Finally, NWs were removed from the substrate and solved in ethanol by sample sonication during a few seconds. Solution concentration was estimated to be between 10<sup>5</sup> and 10<sup>6</sup> NWs per milliliter.

Scanning electron microscopy (SEM) images (Figures 1(a)–1(c)), obtained at a 10 kV operating voltage, show high NW density with fairly uniform lengths and diameters. Cross-section images (Figures 1(b) and 1(c)) reveal that obtained NWs are about  $9 \pm 1 \mu\text{m}$  long and present tip and base diameters of  $58 \pm 6 \text{ nm}$  and  $131 \pm 13 \text{ nm}$ , respectively, where data are obtained from 30 NWs on the oxidized Cu foil and errors are given at a 95% confidence level. NW growth mechanism has been studied by other authors<sup>18,20–22</sup> suggesting that CuO NW growth is based on Cu ion diffusion from the Cu foil through dislocations in the grain boundaries of a thick polycrystalline cuprous oxide (Cu<sub>2</sub>O) layer formed at an early stage of the thermal treatment. Since the growth mechanism is fed by the vertical diffusion of Cu ions

<sup>a)</sup> Author to whom correspondence should be addressed. Electronic mail: [antonio.garciamarin@uam.es](mailto:antonio.garciamarin@uam.es)

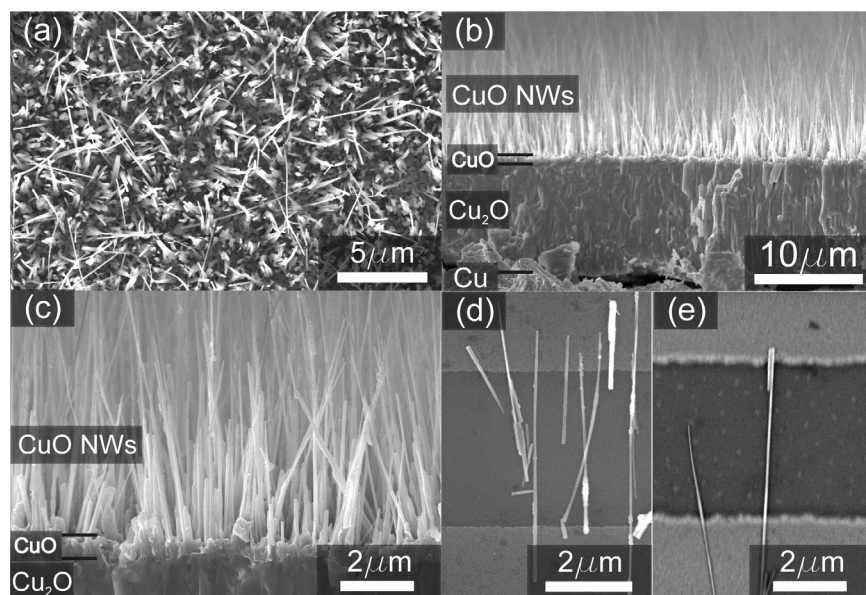


FIG. 1. SEM top (a) and cross-section view (b,c) of a Cu foil at different magnifications containing NWs thermally grown for 1 h. (d,e) Result of the dielectrophoretic alignment of CuO NWs on AZO electrodes.

along the NW in air ambient, some tapering effects can be expected. The presence of the  $\text{Cu}_2\text{O}$  layer is proved using energy-dispersive X-ray (EDX) spectroscopy studies in the SEM characterization. Results show the existence of a  $10\ \mu\text{m}$  thick layer with Cu and O concentrations of 67% and 33%, respectively, which match the stoichiometry of the  $\text{Cu}_2\text{O}$  phase. Due to interfacial stresses induced by the large differences in crystal structure and thermal expansion coefficients between the  $\text{Cu}_2\text{O}$  and the substrate, this layer tends to peel off from the substrate after cooling down, releasing a self-standing layer which contains the NWs.<sup>20</sup> Figure 1(b) shows a crack caused by this effect at the interface between Cu and  $\text{Cu}_2\text{O}$ . Atop this layer, small CuO grains with an average  $0.5\ \mu\text{m}$  size perform as nucleation centers for the NW growth (Figure 1(c)).<sup>21</sup>

X-ray diffractograms of an oxidized sample and the untreated Cu foil were obtained in  $\theta$ - $2\theta$  mode (Figure 2). Diffraction peaks corresponding to the Cu,  $\text{Cu}_2\text{O}$ , and CuO phases were identified from the powder diffraction files (#04-009-2090, #04-007-9767, and #04-008-8209, respectively) of the International Centre for Diffraction Data (ICDD). It can be seen that the original Cu foil presents a polycrystalline

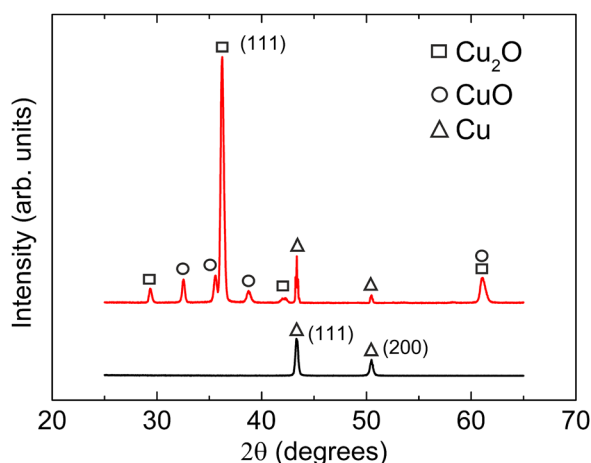


FIG. 2. XRD diffractograms obtained before (bottom line) and after thermal oxidation (top line) of the Cu foil.

structure, showing preferential orientation along (111) and (200) plane directions. After oxidation, the strongest peak corresponds to the  $\text{Cu}_2\text{O}$  (111) plane whose origin is related to the layer built on top of the foil at the early stages of the process. This layer is also polycrystalline as suggested by the other  $\text{Cu}_2\text{O}$  phase reflections present in the diffractogram. On the other hand, all CuO peaks can be indexed using the C2/c space group of the monoclinic structure. Cu is still observable on the oxidized surface because x-rays can penetrate several micrometers through the surface.

The electro-optical characteristics of the NWs are extracted from the following procedure. A  $50\ \text{nm}$  thick AZO film is deposited on a  $\text{SiO}_2(200\ \text{nm})/\text{Si}$  substrate by radio-frequency magnetron sputtering from a 99.999% pure ZnO w/2%  $\text{Al}_2\text{O}_3$  target and Ar plasma at a deposition temperature of  $300^\circ\text{C}$ . The film has a Hall resistivity of  $4 \times 10^{-3}\ \Omega\cdot\text{cm}$ , a mobility of  $4.5\ \text{cm}^2/\text{V}\cdot\text{s}$ , and an electron concentration of  $3 \times 10^{20}\ \text{cm}^{-3}$ . Parallel AZO electrodes with a  $4\ \mu\text{m}$  spacing are defined by optical lithography and chemical etching for DEP experiments. DEP is performed to align the NWs perpendicularly to the electrodes by applying an AC signal of a  $100\ \text{kHz}$  frequency and an  $8\ \text{V}$  peak voltage between electrodes. Resultant NW density on the electrodes was about 65–80 NWs per millimeter length. After DEP process, samples were annealed at  $170^\circ\text{C}$  for 30 s in air ambient to improve the electrical contact and the mechanical resistance of the junctions between the NWs and the AZO electrodes. After the annealing, the structure shows high stability in liquids which enables surface cleaning to get rid of the rests of organic solvents used in the DEP process.

The current-voltage characteristic between electrodes is measured after the processing. The curves present a rectifying behavior likely induced by the n-p-n double junction between AZO and the CuO NW (Figure 3(a)). In fact, if CuO NWs are replaced by ZnO NWs, the device exhibits non-rectifying behavior due to the n-type doping type of ZnO NWs. Moreover, to find out the doping type of the CuO NW, a simple experiment is performed following the procedure described by Han *et al.*<sup>23</sup> based on the surface chemisorption of water molecules. A sample is prepared using CuO NWs

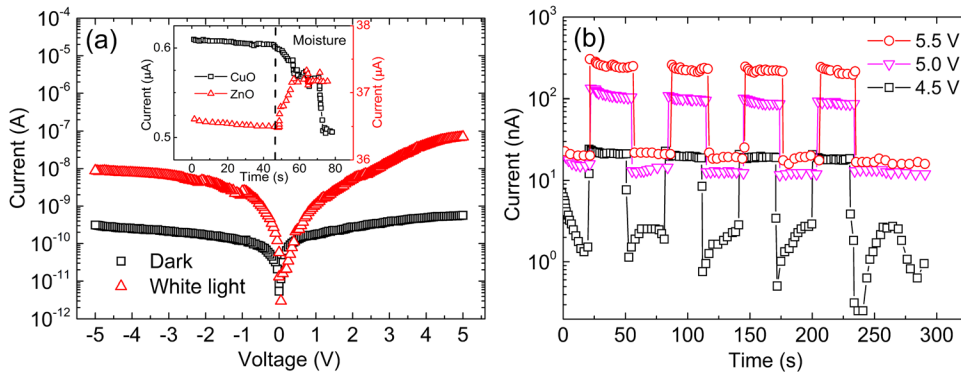


FIG. 3. (a) I-V curves measured in darkness (black squares) and under white light illumination (red triangles). Inset: moisture measurement performed on CuO NWs (black squares) and ZnO NWs (red triangles) to determine doping type. (b) Current transients obtained under pulsed illumination taken at bias voltages of 4.5, 5.0, and 5.5 V.

dispersed on pre-patterned AZO interdigitated electrodes with  $250\ \mu\text{m}$  spacing. For the sake of comparison, a sample is prepared by drop-casting ZnO NWs on a pattern with the same geometry. Both samples are biased at 5 V using an external power supply to measure the current variations between electrodes when the samples are exposed to the water vapor supplied by an ultrasonic humidifier. As the humidity rose up after turning on the apparatus, the current from the ZnO NWs suddenly increases, whereas the signal from the CuO NWs decreases (inset of Figure 3(a)). The results confirm that the surface dissociation of water molecules on the NW surface releases electrons to the NW volume, enhancing the conductivity for the ZnO NWs, but reducing it for the CuO NWs. Furthermore, it corroborates that the CuO NW behaves as a p-type semiconductor material and that the rectifying behavior observed in the AZO/CuO NW/AZO heterojunction is related to the formation of a double p-n junction at the NW ends.

The current delivered by the AZO/CuO NW/AZO structure noticeably increases when it is illuminated with a halogen lamp of  $4.54\ \text{mW}/\text{cm}^2$  power density. Furthermore, the response obtained at constant bias voltages (Figure 3(b)) shows fast transients except for the erratic behavior of the dark current at 4.5 V caused by the noise level of the setup. Due to the different doping type, a space charge region (SCR) is expected to be built at the junctions between the NW and the AZO electrodes maximizing the electric field strength and contributing to promptly separate carriers upon photogeneration. In semiconductor photodetector theory, time response in p-n structures is predicted to be limited by transit time across SCRs and by diffusion times in the neutral regions around the junction.<sup>24</sup> However, in practice, these theoretical times are usually shorter than the charge and discharge times of the parasitic capacitances.<sup>25</sup> On the other hand, in detectors with uniform electric field profiles, i.e. photoconductive-type detectors, time response is limited by the generation-recombination times of the photocarriers which, in the presence of trapping centers, can become very long.<sup>26</sup> Thus, the fast response found in the structure under study may be related to the alignment of p-type NWs between n-type electrodes which yields series-opposing photodiodes capable of minimizing the effect of trapping centers. Another complementary explanation of the fast response is that, unlike other metal oxide NWs, surface states in CuO may act as recombination centers, helping to speed up charge recombination after illumination at neutral

regions. Femtosecond transient absorption spectroscopy studies have also demonstrated relaxation times in the picosecond range in p-type CuO NWs, which somehow proves the fast dynamic behavior of photocarriers in this material.<sup>27</sup>

To further investigate the time response characteristic, the structure is illuminated with  $100\ \mu\text{s}$  pulses from a red (peak wavelength = 630 nm, power density =  $0.76\ \text{mW}/\text{cm}^2$ ) light emitting diode (LED) at a repetition rate of 1 kHz using a function generator. The device is connected to a 5 V external power supply and a load resistance ( $R_L$ ) to measure the photocurrent pulses in a Tektronix TDS210 oscilloscope. Under these experimental conditions, a minimum load resistance of  $40\ \text{k}\Omega$  is necessary to monitor the photocurrent signal in the oscilloscope. A responsivity value of  $9.8\ \text{A}/\text{W}$  is estimated at a  $R_L$  of  $510\ \text{k}\Omega$  and 5 V. Photocurrent pulses, shown in the inset of Figure 4(a), followed first-order exponentials for rise and decay portions of the curve with time constants in the few microsecond level. The value of the time constants reduces as the  $R_L$  diminishes, indicating that the device response may be limited by the resistance-capacitance (RC) of the equivalent circuit. To confirm this, a capacity bridge was used at a 50 mV level and 1 kHz under a DC bias of 5 V. Parallel ( $R_p$ ) and series ( $R_s$ ) resistances were estimated to be  $60\ \text{M}\Omega$  and  $0.024\ \text{M}\Omega$ , respectively. Since  $R_s$  is significantly lower than  $R_p$ , the effect of the latter can be neglected to calculate the RC constant of the circuit according to the diode model shown in the inset of Figure 4(b). The  $R_s$  value has its origin in the AZO electrode resistivity since it hardly changes after NW deposition. Differential capacitance between both electrodes before and after DEP accounts for the contribution of the multiple nanowires to the total capacitance ( $C_{\text{mNW}}$ ) resulting in  $C_{\text{mNW}} = 14\ \text{pF}$ . This capacitance is attributed to the sum of capacitors formed at the contact points between NWs and DEP electrodes. The large number, around 500 NWs observed by optical microscopy, leads to an estimated value of 28 fF for each NW which is similar to 21 fF, previously reported in the bibliography for a single CuO NW.<sup>19</sup> The RC product, calculated from  $(R_s + R_L) \cdot C_{\text{mNW}}$ , is represented against  $R_L$  in red dashed lines in Figures 4(a) and 4(b), showing a fairly good correlation between the model and the experimental data. This means that, unlike other metal oxide NW photodetectors, the time response is mainly limited by the RC product without traces of surface persistent effects. The small misfit between the model curve and the experimental data is attributed to parasitic capacitances between the AZO electrodes and the floating substrate through the



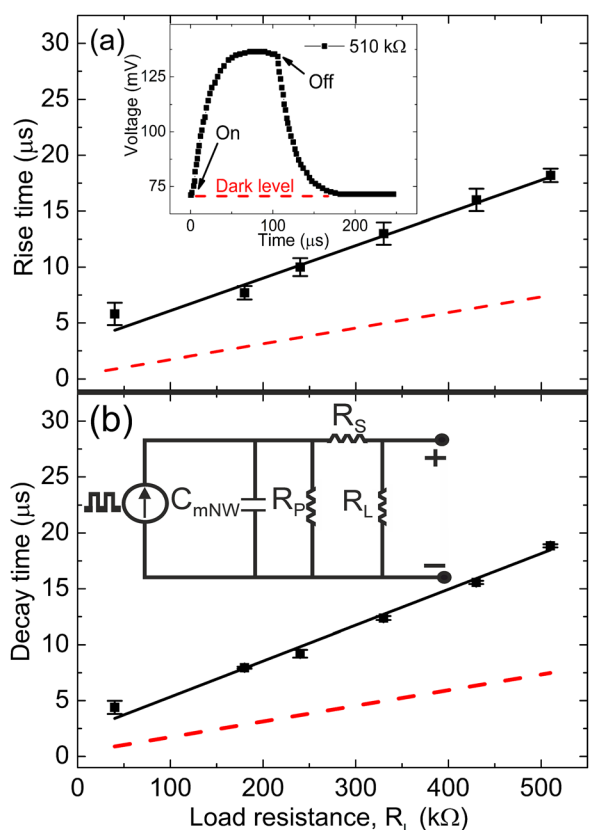


FIG. 4. (a) Rise time as function of load resistance. Inset: a registered pulse obtained at  $R_L = 510 \text{ k}\Omega$ . (b) Decay time as function of load resistance. Inset: equivalent circuit.

dielectric layer. The capacitance between the Si substrate and the AZO electrodes has been measured in different devices using a backside contact. Values between 20 and 55 pF are, respectively, found in depletion and accumulation biasing conditions for the 200 nm thick  $\text{SiO}_2$  layer. Despite vertical conduction through the oxide is measured to be null, these capacitors associated to the AZO electrodes may slow down the response speed since their capacitance is comparable or even larger than  $C_{\text{mNW}}$ .

In conclusion, AZO/CuO NW/AZO heterojunctions have been built using cost-effective Cu foil oxidation for NW synthesis, and CMOS-compatible DEP for NW alignment. Time response has been found to be in the  $\mu\text{s}$ -range without signs of persistent effects. The reduction of device parasitics can lead to a further improvement of the device speed. These results may contribute to the understanding of the p-type CuO NW characteristics as well as to establish

standard procedures for the integration of NW-based devices in nanoelectronics.

Authors thank Pedro Rodríguez for technical assistance and the financial support of Comunidad de Madrid and MINECO through the R+D S2009/PPQ-1642 program and the TEC2010-20796 project, respectively.

- <sup>1</sup>C. Soci, A. Zhang, B. Xiang, S. A. Dayeh, D. P. R. Aplin, J. Park, X. Y. Bao, Y. H. Lo, and D. Wang, *Nano. Lett.* **7**, 1003 (2007).
- <sup>2</sup>X. Li, Y. Wang, Y. Lei, and Z. Gu, *RSC. Adv.* **2**, 2302 (2012).
- <sup>3</sup>I.-S. Hwang, S.-J. Kim, J.-K. Choi, J.-J. Jung, D. J. Yoo, K.-Y. Dong, B.-K. Ju, and J.-H. Lee, *Sens. Actuators B* **165**, 97 (2012).
- <sup>4</sup>M.-W. Ahn, K.-S. Park, J.-H. Heo, D.-W. Kim, K. J. Choi, and J.-G. Park, *Sens. Actuators B* **138**, 168 (2009).
- <sup>5</sup>J. Tang, Z. Huo, S. Brittman, H. Gao, and P. Yang, *Nat. Nanotechnol.* **6**, 568 (2011).
- <sup>6</sup>M. Mashock, K. Yu, S. Cui, S. Mao, G. Lu, and J. Chen, *Appl. Mater. Interfaces* **4**, 4192 (2012).
- <sup>7</sup>C. G. Núñez, J. L. Pau, E. Ruiz, A. G. Marín, B. J. García, J. Piqueras, G. Shen, D. S. Wilbert, S. M. Kim, and P. Kung, "Enhanced fabrication process of zinc oxide nanowires for optoelectronics," *Thin Solid Films* (submitted).
- <sup>8</sup>Y. Liu, J.-H. Chung, W. K. Liu, and R. S. Ruoff, *J. Phys. Chem. B* **110**, 14098 (2006).
- <sup>9</sup>D. Wang, R. Zhu, Z. Zhou, and X. Ye, *Appl. Phys. Lett.* **90**, 103110 (2007).
- <sup>10</sup>K. Liu, M. Sakurai, M. Liao, and M. Aono, *J. Phys. Chem. C* **114**, 19835 (2010).
- <sup>11</sup>L. Guo, H. Zhang, D. Zhao, B. Li, Z. Zhang, M. Jiang, and D. Shen, *Sens. Actuators B* **166–167**, 12 (2012).
- <sup>12</sup>B. J. Hansen, N. Kouklin, G. Lu, I.-K. Lin, J. Chen, and X. Zhang, *J. Phys. Chem. C* **114**, 2440 (2010).
- <sup>13</sup>T. Ito, H. Yamaguchi, T. Masumi, and S. Adachi, *J. Phys. Soc. Jpn.* **67**, 3304 (1998).
- <sup>14</sup>S. B. Wang, C. H. Hsiao, S. J. Chang, K. T. Lam, K. H. Wen, S. C. Hung, S. J. Young, and B. R. Huang, *Sens. Actuators A* **171**, 207 (2011).
- <sup>15</sup>J. Xu, J.-L. Sun, J. Wei, and J. Xu, *Appl. Phys. Lett.* **100**, 251113 (2012).
- <sup>16</sup>A. S. Ethiraj and D. J. Kang, *Nanoscale Res. Lett.* **7**, 70 (2012).
- <sup>17</sup>G. Cheng, S. Wang, K. Cheng, X. Jiang, L. Wang, L. Li, Z. Du, and G. Zou, *Appl. Phys. Lett.* **92**, 223116 (2008).
- <sup>18</sup>A. M. B. Gonçalves, L. C. Campos, A. S. Ferlauto, and R. G. Lacerda, *J. Appl. Phys.* **106**, 034303 (2009).
- <sup>19</sup>L. Liao, Z. Zhang, B. Yan, Z. Zheng, Q. L. Bao, T. Wu, C. M. Li, Z. X. Shen, J. X. Zhang, H. Gong, J. C. Li, and T. Yu, *Nanotechnology* **20**, 085203 (2009).
- <sup>20</sup>C. H. Xu, C. H. Woo, and S. Q. Shi, *Chem. Phys. Lett.* **399**, 62 (2004).
- <sup>21</sup>J. T. Chen, F. Zhang, J. Wang, G. A. Zhang, B. B. Miao, X. Y. Fan, D. Yan, and P. X. Yan, *J. Alloys Compd.* **454**, 268 (2008).
- <sup>22</sup>R. Mema, L. Yuan, Q. Du, Y. Wang, and G. Zhou, *Chem. Phys. Lett.* **512**, 87 (2011).
- <sup>23</sup>J.-W. Han, B. Kim, N. P. Kobayashi, J. Li, and M. Meyyappan, *Appl. Phys. Lett.* **101**, 142110 (2012).
- <sup>24</sup>S. M. Sze and K. Kwok, *Physics of Semiconductor Devices*, 3rd ed. (Wiley, New Jersey, 2007).
- <sup>25</sup>J. L. Pau, E. Monroy, E. Muñoz, F. Calle, M. A. Sánchez-García, and E. Calleja, *Electron. Lett.* **37**, 239 (2001).
- <sup>26</sup>R. H. Bube, *Photoconductivity of Solids* (Krieger, New York, 1978).
- <sup>27</sup>A. Othonos and M. Zervos, *Nanoscale Res. Lett.* **6**, 622 (2011).